Int Urogynecol J (2015) 26:685–691
DOI 10.1007/s00192-014-2571-y

ORIGINAL ARTICLE

Label-free, three-dimensional multiphoton microscopy of the connective tissue in the anterior vaginal wall

Michal Sikora · David Scheiner · Cornelia Betschart · Daniele Perucchini · José María Mateos · Anthony di Natale · Daniel Fink · Caroline Maake

Received: 12 May 2014 / Accepted: 4 November 2014 / Published online: 25 November 2014

Abstract
Introduction and hypothesis Multiphoton microscopy (MPM) is a nonlinear, high-resolution laser scanning technique and a powerful approach for analyzing the spatial architecture within tissues. To demonstrate the potential of this technique for studying the extracellular matrix of the pelvic organs, we aimed to establish protocols for the detection of collagen and elastin in the vagina and to compare the MPM density of these fibers to fibers detected using standard histological methods.
Methods Samples of the anterior vaginal wall were obtained from nine patients undergoing a hysterectomy or cystocele repair. Samples were shock frozen, fixed with formaldehyde or Thiel's solution, or left untreated. Samples were imaged with MPM to quantify the amount of collagen and elastin via second harmonic generation and autofluorescence, respectively. In six patients, sample sections were also histologically stained and imaged with brightfield microscopy. The density of the fibers was quantified using the StereoInvestigator and Cavalieri software.
Results With MPM, collagen and elastin could be visualized to a depth of 100 μm, and no overlap of signals was detected. The different tissue processing protocols used did not result in significantly different fiber counts after MPM. MPM-based fiber quantifications are comparable to those based on conventional histological stains. However, MPM provided superior resolution, particularly of collagen fibers.
Conclusions MPM is a robust, rapid, and label-free method that can be used to quantify the collagen and elastin content in thick specimens of the vagina. It is an excellent tool for future three-dimensional studies of the extracellular matrix in patients with pelvic organ prolapse.

Keywords Multiphoton microscopy · Collagen · Elastin · Vagina · Pelvic organ prolapse

Introduction

The integrity of the vagina and its supportive connective tissues is essential for maintaining the normal anatomic position of the pelvic organs. The connective tissue underlying the vagina contains relatively few cells, mainly fibroblasts, which produce components of the extracellular matrix (ECM). The ECM contains fibrillar components such as collagen and elastin that are embedded in a non-fibrillar ground substance consisting of non-collagenous glycoproteins, proteoglycans, and hyaluronan [1]. Using molecular, biochemical, histological, and immunohistochemical approaches, numerous studies have provided strong evidence that ECM synthesis, repair, and remodeling is impaired in women with pelvic organ prolapse (POP) [2].

There is still no clear evidence of changes in the three-dimensional (3-D) organization of pelvic floor connective tissue fibers because none of the "classical" examination techniques is suitable for visualizing the spatial distribution of ECM constituents in thick specimens. However, as shown in other clinical conditions including chronic obstructive pulmonary disease, aortic aneurysms, or lupus erythematosus, specific information about the architecture of the connective tissue fibers and alterations in the connective tissue fibers

Michal Sikora and David Scheiner contributed equally to this study.

M. Sikora (✉) · D. Scheiner · C. Betschart · D. Perucchini · D. Fink
Department of Gynecology, University Hospital Zurich,
Frauenklinikstrasse 10, 8091 Zurich, Switzerland
e-mail: michal.sikora@usz.ch

A. di Natale · C. Maake
Institute of Anatomy, University of Zurich,
Winterthurerstrasse 190, 8057 Zurich, Switzerland

J. M. Mateos
Center for Microscopy and Image Analysis, University of Zurich,
Winterthurerstrasse 190, 8057 Zurich, Switzerland

could lead to a better understanding of disease pathoetiology [3–5].

Multiphoton microscopy (MPM) is a nonlinear, high-resolution laser scanning technique that allows 3-D investigations of thick biological samples. Thus, MPM has recently emerged as a significant tool for both in vitro and in vivo studies in, e.g., neuroscience, immunology, and cancer research [6]. Multiphoton excitation allows for several powerful imaging techniques; the two most commonly used procedures are two-photon excitation fluorescence and second harmonic generation (SHG) microscopy [6, 7]. These methods excite the characteristic UV absorption bands of endogenous fluorophores, including elastic fibers (by two-photon excitation autofluorescence) and collagen fibers (by SHG), without the need for labeling [8]. Compared to other microscopy techniques, MPM substantially increases the maximum imaging depth from a few tenths of a micrometer to nearly 1 mm in certain tissue types, such as brain [9]. Further advantages—especially compared to confocal microscopy—are reduced scattering and absorption due to the longer excitation wavelengths and significantly reduced phototoxicity and photobleaching in out-of-focus regions [8]. In addition, MPM allows not only for qualitative but also for quantitative analysis of collagen and elastin fibers [10, 11], as recently shown for, e.g., the dermis, arteries, cartilage, or heart [12–14].

These features and distinct advantages of MPM motivated us to investigate the 3-D structure of the vaginal ECM by MPM. However, before clinically relevant studies can be completed, several basic parameters have to be established. Thus, our present study had two objectives: (1) to establish a suitable procedure for preparing vaginal tissue for MPM and (2) to evaluate the potential of MPM in visualizing the 3-D pattern of collagen and elastic fibers in the anterior vaginal wall in comparison to conventional histological staining methods.

Materials and methods

This project was performed at the Department of Gynecology at the University Hospital Zurich in collaboration with the Institute of Anatomy at the University of Zurich.

Patients

Between October 2010 and January 2012, full-thickness samples of the anterior vaginal wall were obtained using a standardized procedure. Samples were collected from the anterior vaginal apex in four patients who underwent hysterectomy for benign gynecological conditions without POP and from the anterior vaginal wall, 7 cm cranially to the hymen, in five patients who underwent cystocele repair (anterior colporrhaphy) for cystocele stage II or higher according to the Pelvic Organ Prolapse Quantification system (POP-Q, samples were taken from an area as close as possible to the vaginal apex) [15]. The indication for hospitalization and surgery was given according to the gynecological diagnosis. Exclusion criteria were patients under 18 years of age, pregnancy and lactation, current gynecological cancers, neoplasm in the pelvic or anogenital area, abdominal neoplasm, florid local infections including genital infection with the human papilloma virus, or use of steroids or methotrexate (e.g., in rheumatoid disease). Written informed consent was obtained from each enrolled patient. Ethical approval was obtained from the local Cantonal Ethics Committee (StV 11/2009). This study is registered with ClinicalTrials.gov, number NCT01042470.

Tissue preparation

Specimens were obtained and prepared in the operating room immediately. For patients 1–3, specimens were cut using a standardized method into four identical full-thickness pieces that were treated with one of the following methods: (1) fixation in 4 % formaldehyde (FA) for 12 h at 4 °C followed by washing with phosphate-buffered saline (PBS) pH 7.2, (2) fixation in Thiel's solution [16] for 12 h at 4 °C followed by washing with PBS, (3) shock freezing in liquid nitrogen, storage for 12 h at −80 °C and defrosting just before sectioning and (4) not treating the tissue, keeping it on blue ice, and cutting it within 5 h. For MPM, all samples were sectioned in a standardized manner with the same tissue orientation into four 500-μm-thick slices (Tissue Chopper, Mickle Laboratory Engineering, Guildford, UK), embedded with glycerol gel melting medium containing 1,4-diazabicyclo[2.2.2]octane (DABCO, Dako, Glostrup, Denmark), and covered with a CoverWell imaging chamber (Invitrogen, Zug, Switzerland).

In patients 4–9, specimens were fixed with 4 % FA for 12 h at 4 °C, washed in PBS, and divided into two full-thickness pieces. Subsequently, one piece was sectioned for MPM as described above taking care to standardize tissue orientation. The second piece was frozen and cryocut in a standardized manner with the same tissue orientation into 6-μm sections for histological staining.

Multiphoton laser scanning microscopy

Three-dimensional stacks of 167×167×50 μm were acquired using a multiphoton laser scanning microscope equipped with a Ti:sapphire laser (Olympus Fluoview 1000 MPE, Volketswil, Switzerland) at a wavelength of 950 nm and a ×25 water objective (Olympus, NA 1.05). Standardized imaging was performed within the lamina propria (submucosa), i.e., between the readily recognizable epithelium and the smooth muscle layer of the vaginal wall. Collagen fibers were

Table 1 Basic characteristics of patients including body mass index (BMI)

Patient number	Age (years)	BMI (kg/m^2)	Weight (kg)	Height (m)	Menopausal status	Parity	Cystocele (POP-Q)
1	68.5	22.8	57.0	1.58	Postmenopausal	2	None
2	46.9	24.6	68.5	1.67	Premenopausal	2	Cystocele II
3	51.8	20.0	50.0	1.58	Premenopausal	1	Cystocele II
4	68.4	21.3	52.4	1.57	Postmenopausal	2	None
5	40.3	30.0	74.9	1.58	Premenopausal	3	None
6	62.6	23.1	57.0	1.57	Postmenopausal	2	Cystocele II
7	68.6	26.5	74.0	1.67	Postmenopausal	0	Cystocele II
8	49.0	20.1	54.8	1.65	Premenopausal	2	Cystocele III
9	40.2	27.0	69.0	1.60	Premenopausal	0	None

detected by SHG (475 nm) and elastin fibers by autofluorescence (515–560 nm). For each patient, four 3-D stacks were obtained (one from each tissue slice) per MPM treatment protocol.

Brightfield microscopy

Four sections (100 mm distance on the z-axis) per patient 4–9 were stained histologically according to routine procedures with either van Gieson (to visualize collagen fibers) or resorcin fuchsin (for elastin fibers) and subjected to brightfield microscopy with an upright Leica LX microscope using a ×40 oil immersion objective (NA 1.25) attached to a CCD camera (Leica DFC 350, Heerbrugg, Switzerland) [17] to acquire a two-dimensional (2-D) 167×167 μm image.

Analysis

Three-dimensional data of multiphoton stacks were visualized with the Imaris 7.2.1 software (Bitplane, Zurich, Switzerland) and collagen and elastic fibers were quantified within three planes in 10-μm intervals on the z-axis using the StereoInvestigator software and the Area Fraction Fractionator probe (MBF Bioscience, Williston, VT, USA). The density of the collagen and elastin fibers was calculated using previously described algorithms [18]. The density of the collagen and elastin fibers in 2-D histological images was determined with the Cavalieri estimator software (MBF Bioscience) within a 70×70 μm point grid according to previously published methods [19]. Statistical analysis was completed using the Intercooled Stata 12.0 software (StataCorp LP, College Station, TX, USA) with the Wilcoxon signed rank test and the Kruskal-Wallis test as appropriate. *P* values below 0.05 indicate statistical significance (two-sided).

Results

Table 1 shows the basic characteristics of the nine patients.

With MPM imaging, vaginal structures to a maximal depth of 100 μm were visualized. In none of the tested pretreatment protocols did 3-D images resolved with MPM imaging show an overlap of anisotropic collagen and isotropic elastin signals in the submicron range, which allowed simultaneous and label-free detection of both fiber types in the vaginal wall (Fig. 1). Three-dimensional images revealed an extensive

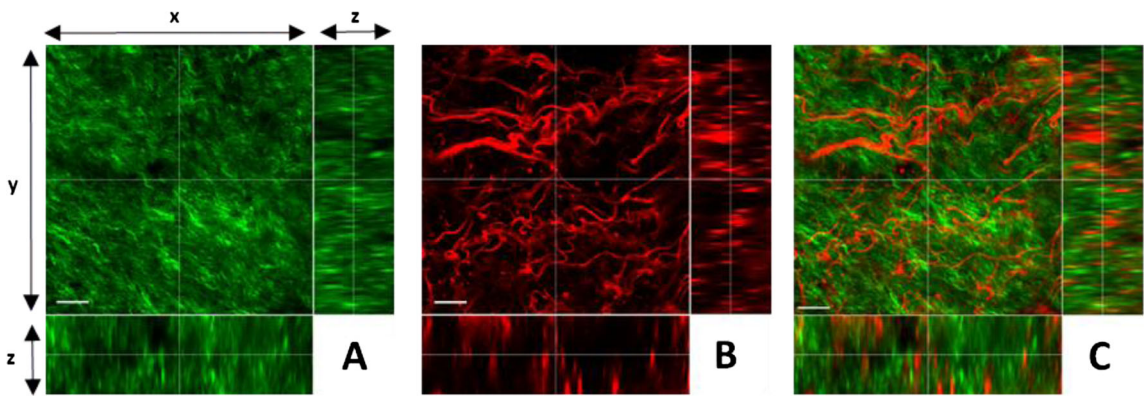

Fig. 1 Three-dimensional multiphoton laser scanning microscopy of the lamina propria of the anterior vaginal wall (x-, y-, and z-axis). **a** Collagen fibers (SHG, in *green*). **b** Elastic fibers (autofluorescence, in *red*). **c** Overlay. *Scale bar* represents 20 μm

network of collagen and elastic fibers within the subepithelial connective tissue layer of the lamina propria.

Table 2 shows the volumes of the collagen and elastin fibers assessed from the 3-D MPM stacks of the samples from patients 1–3 that had been subjected to fixation with either 4 % FA, Thiel's solution, shock freezing, or no treatment (native tissue). Measurements were not significantly different between the four pretreatment protocols in any of the patients ($P>0.05$).

The suitability of MPM for studies of the vaginal ECM was further evaluated by comparison with standard histology techniques and brightfield microscopy. As detailed in Table 3, a statistically significant difference in the volumes of collagen or elastin was not observed in any of the patients or between the MPM-based and histology-based analyses ($P>0.05$). However, compared to histological staining methods, MPM images showed collagen fibers at a higher resolution (Fig. 2).

Discussion

We present here for the first time a methodological evaluation of MPM for future, detailed 3-D analyses of collagen and elastic fibers within the vaginal wall. Notably, it was not the intention of our study to compare the collagen and elastin contents of patients with POP versus controls. Women with different medical conditions were included in our study for the sole purpose of examining the applicability of the method to different collectives.

Frequently, fresh tissue is used to study collagen and elastin fibers by MPM [20–23], but this is not always practical in a clinical setting. However, the suitability of formalin fixation and freezing for MPM of the ECM has previously been reported for various tissues, including lung, aorta, and skin [3, 5, 24, 25]. To set the stage for our further investigations, we initially confirmed these data for the vagina, showing for the first time that tissue preservation by fixation or snap freezing had no significant impact on quantitative MPM evaluations of either collagen or elastin fibers in the lamina propria. The observation that MPM allows for reliable fiber measurements in untreated vaginal samples suggests that MPM can be used to perform additional biomechanical studies of the ECM. Once we concluded that all of the investigated tissue pretreatments were suitable for MPM measurements of these two fiber types in the vagina, we used formalin-fixed samples for subsequent studies because of two reasons: (1) generally, tissue preservation by fixation eliminates the problem of imaging within a short time frame and (2) more specifically, formalin is always available in the operating room.

While our fixation protocols were well applicable for MPM analyses of collagen and elastin, other procedures may interfere with MPM. This applies, e.g., to glutaraldehyde fixation, commonly used for histological staining and electron microscopy, which leads to an enhancement of autofluorescence and axial shrinkage of collagen [26, 27].

Under the chosen MPM conditions (excitation 950 nm), we observed no overlap between the SHG (emission at 475 nm) and two-photon autofluorescence (emission at 515–560 nm) images, which indicates the specificity of the signals obtained [8]. Similar MPM modalities, i.e., 940 nm excitation, have been applied successfully to detect collagen and elastin in ex vivo breast tissues [28]. In several other tissues, e.g., skin, arteries, or brain, other wavelength ranges have been used for specific SHG imaging of collagen (excitation 780–860 nm, emission 390–430 nm) and two-photon autofluorescence of elastin (excitation 760–850 nm, emission 435–697 nm) [4, 20, 22, 24, 29].

We were also interested in comparing our MPM measurements to those generated with conventional microscopy techniques. Most previous microscopic investigations of connective tissue of POP samples used either histological staining or immunohistochemistry to detect and quantify collagen and/or elastin [2, 30]. Immunohistochemical methods are advantageous because they can distinguish between different collagen

Table 2 Comparison of collagen and elastin density in MPM images in samples taken from patients 1–3

	Patient 1		Patient 2		Patient 3	
	Collagen	Elastin	Collagen	Elastin	Collagen	Elastin
4 % FA	67.4 (51.4–69.5)	11.8 (9.7–16.7)	54.9 (54.9–82.0)	16.7 (11.8–22.2)	43.7 (28.8–51.5)	21.0 (13.2–22.2)
Thiel's	59.1 (45.2–80.6)	13.2 (11.1–13.2)	51.4 (44.5–61.8)	12.5 (12.5–10.4)	61.1 (50–78.5)	20.2 (18.1–32.0)
Shock frozen	58.4 (57.0–79.2	16.7 (9.7–18.8)	57 (51.4–70.9)	11.8 (11.8–24.3)	50 (50–55.6)	20.8(15.3–24.3)
Untreated	50.7 (38.9–55.6)	5.6 (3.5–13.9)	60.5 (59.8–79.2)	24.3 (16–29.9)	65.3 (54.9–85.5)	20.2 (20.2–20.8)
P value	0.28	0.46	0.48	0.28	0.53	0.68

The following four tissue processing methods were compared: fixation with 4 % FA, fixation with Thiel's solution (Thiel's), shock freezing, and no treatment (untreated). For each patient and processing method, four MPM image stacks were analyzed using the StereoInvestigator software. Data are expressed as the median (minimum–maximum) of the total tissue volume visualized. *P* values are given for the comparison between all of the pretreatments for each fiber type per patient (Kruskal-Wallis equality of populations rank test)

Table 3 Comparison of the amount of collagen and elastin fibers by MPM imaging versus histologically stained and visualized using brightfield microscopy (Histo) in tissue sections from patients 4–9

Patient number	4		5		6		7		8		9	
Detection method	MPM	Histo	MPM	Histo	MPM	Histo	MPM	Histo	MPM	Histo	MPM	Histo
Collagen, % (min.–max.)	51.7 (47.6–53.7)	54.6 (44.3–67.0)	65.1 (62.4–65.5)	62.6 (60.2–67.8)	64.2 (53.9–73.1)	50.7 (46.7–52.6)	58.9 (56.4–63.9)	49.9 (45.1–59.8)	57.6 (54.8–59.5)	62.2 (53.4–66.6)	58.7 (54.9–65.7)	66.2 (59.0–71.8)
P-value	0.4652		1.0		0.1441		0.2733		0.2733		0.4652	
Elastin % (Min.-Max.)	21.2 (17.5–24.1)	23.1 (18.3–26.7)	15.4 (13.1–17.6)	10.4 (9.6–12)	30.0 (28.8–30.7)	32.7 (32.7–33.9)	16.0 (15.8–16.9)	18.7 (17.1–21.9)	15.8 (12.7–17.6)	13.2 (12.4–16.4)	17.5 (13.4–22.1)	20.7 (16.4–24.3)
P value	0.1441		0.0679		0.0679		0.1441		0.4652		0.0679	

For MPM analyses, four image stacks were measured per patient using the StereoInvestigator software. For histology analyses, four sections were measured per patient using the Cavalieri estimator software. Data are expressed as the median (minimum–maximum) of the section's density. *P* values are given for the comparison between MPM and histological staining for each patient (Wilcoxon signed rank test)

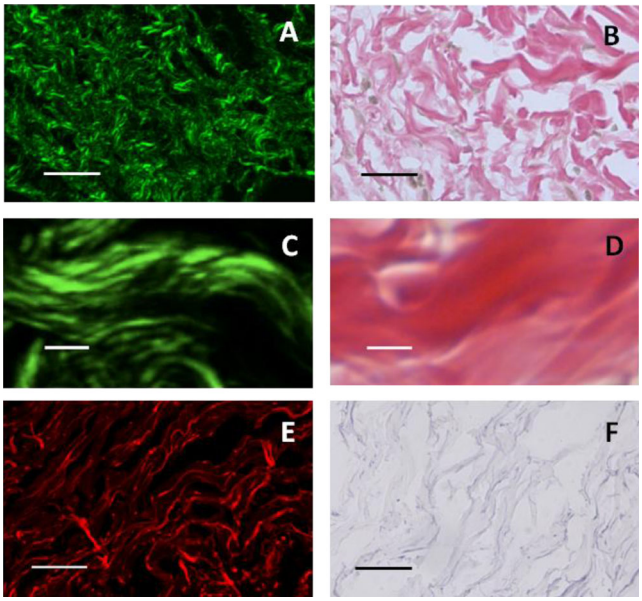

Fig. 2 Comparison of the two visualization methods. MPM of collagen (**a** and **c**, SHG) and elastic fibers (**e**, autofluorescence). Brightfield microscopy images of collagen (**b** and **d**, van Gieson stain) and elastic fibers (**f**, resorcin fuchsin stain). *Scale bars* in **a**, **b**, **e**, and **f** represent 30 μm and in **c** and **d** represent 5 μm

subtypes. However, because no single antibody cross-reacts with all collagen types present in the ECM of the vagina [2, 31, 32], this method is not an optimal reference for MPM, which only detects total collagen. We therefore decided to focus on a comparison with standard histology stains. Our data showed that vaginal collagen and elastin quantifications based on MPM are comparable to those obtained with conventional histology ($P>0.05$). This is in accordance with previous nonquantitative studies that also reported a correlation between MPM and histology stains for collagen and elastic fibers in different tissues [11, 24, 33–35]. However, it is important to stress that a higher resolution was obtained with MPM, especially of collagen fibers, in the vagina than with histology stains.

While MPM analyses of ECM fibers also have some limitations (including the expensive equipment, problems related to highly scattering tissues, or the inability to distinguish between different collagen types), we anticipate that future studies dealing with the vaginal ECM will strongly benefit from MPM. In contrast to other microscopy methods, it offers a unique possibility of precisely examining the global collagen and elastin content in an unprecedentedly large (3-D) sample volume without the need for labeling procedures. This will lead to new insight into the details of the architectural arrangement of collagen and elastin networks in pelvic structures, allowing, e.g., for the assessment of the lengths, orientations, or thickness of the fibers. Current studies are now devoted to systematic MPM investigations of the changes in the ECM in patients with POP.

Acknowledgments The authors would like to thank Theresa Lehmann and Charlotte Burger for technical assistance with the tissue processing and histological staining.

Conflicts of interest None.

References

1. Kerkhof MH, Hendriks L, Brölmann HA (2009) Changes in connective tissue in patients with pelvic organ prolapse–a review of the current literature. Int Urogynecol J Pelvic Floor Dysfunct 20(4):461–474. doi:10.1007/s00192-008-0737-1
2. De Landsheere L, Munaut C, Nusgens B, Maillard C, Rubod C, Nisolle M, Cosson M, Foidart JM (2013) Histology of the vaginal wall in women with pelvic organ prolapse: a literature review. Int Urogynecol J 24(12):2011–2020. doi:10.1007/s00192-013-2111-1
3. Abraham T, Hogg J (2010) Extracellular matrix remodeling of lung alveolar walls in three dimensional space identified using second harmonic generation and multiphoton excitation fluorescence. J Struct Biol 171(2):189–196. doi:10.1016/j.jsb.2010.04.006
4. Zhu X, Lin L, Yu H, Zhuo S, Chen J, Liu J, Wang Y (2012) Visualization of epidermal and dermal alteration in papulonodular mucinosis by multiphoton microscopy. Scanning 35(1):22–27. doi:10.1002/sca.21031
5. Phillippi JA, Green BR, Eskay MA, Kotlarczyk MP, Hill MR, Robertson AM, Watkins SC, Vorp DA, Gleason TG (2014) Mechanism of aortic medial matrix remodeling is distinct in patients with bicuspid aortic valve. J Thorac Cardiovasc Surg 147(3):1056–1064. doi:10.1016/j.jtcvs.2013.04.028
6. Ustione A, Piston DW (2011) A simple introduction to multiphoton microscopy. J Microsc 243(3):221–226. doi:10.1111/j.1365-2818.2011.03532.x
7. Friedl P, Wolf K, von Andrian UH, Harms G (2007) Biological second and third harmonic generation microscopy. Curr Protoc Cell Biol Chapter 4:Unit 4.15. doi:10.1002/0471143030.cb0415s34
8. Schenke-Layland K (2008) Non-invasive multiphoton imaging of extracellular matrix structures. J Biophotonics 1(6):451–462. doi:10.1002/jbio.200810045
9. Theer P, Hasan MT, Denk W (2003) Two-photon imaging to a depth of 1000 microm in living brains by use of a Ti:Al2O3 regenerative amplifier. Opt Lett 28(12):1022–1024
10. Chen XN, Nadiarynkh O, Plotnikov S, Campagnola PJ (2012) Second harmonic generation microscopy for quantitative analysis of collagen fibrillar structure. Nat Protoc 7(4):654–669. doi:10.1038/nprot.2012.009
11. Tong PL, Qin J, Cooper CL, Lowe PM, Murrell DF, Kossard S, Ng LG, Roediger B, Weninger W, Haass NK (2013) A quantitative approach to histopathological dissection of elastin-related disorders using multiphoton microscopy. Br J Dermatol 169(4):869–879. doi:10.1111/bjd.12430
12. Chen J, Zhu X, Xu Y, Tang Y, Xiong S, Zhuo S, Chen J (2014) Stereoscopic visualization and quantification of auricular cartilage regeneration in rabbits using multiphoton microscopy. Scanning 36(5):540–546. doi:10.1002/sca.21153
13. Cui JZ, Tehrani AY, Jett KA, Bernatchez P, van Breemen C, Esfandiarei M (2014) Quantification of aortic and cutaneous elastin and collagen morphology in Marfan syndrome by multiphoton microscopy. J Struct Biol 187(3):242–253. doi:10.1016/j.jsb.2014.07.003
14. Martin TP, Norris G, McConnell G, Currie S (2013) A novel approach for assessing cardiac fibrosis using label-free second harmonic generation. Int J Cardiovasc Imaging 29(8):1733–1740. doi:10.1007/s10554-013-0270-2
15. Bump RC, Mattiasson A, Bø K, Brubaker LP, DeLancey JO, Klarskov P, Shull BL, Smith AR (1996) The standardization of terminology of female pelvic organ prolapse and pelvic floor dysfunction. Am J Obstet Gynecol 175(1):10–17
16. Thiel W (1992) The preservation of the whole corpse with natural color. Ann Anat 174(3):185–195
17. Böck P (ed) (1989) Romeis Mikroskopische Technik, 17th edn. Urban und Schwarzenberg, Munich
18. Howard CV, Reed MG (eds) (1998) Unbiased stereology. BIOS Scientific Publishers, Oxford
19. Gundersen HJ, Jensen EB, Kiêu K, Nielsen J (1999) The efficiency of systematic sampling in stereology–reconsidered. J Microsc 193(Pt 3):199–211
20. Peloquin J, Huynh J, Williams RM, Reinhart-King CA (2011) Indentation measurements of the subendothelial matrix in bovine carotid arteries. J Biomech 44(5):815–821. doi:10.1016/j.jbiomech.2010.12.018
21. Chen H, Liu Y, Slipchenko MN, Zhao X, Cheng JX, Kassab GS (2011) The layered structure of coronary adventitia under mechanical load. Biophys J 101(11):2555–2562. doi:10.1016/j.bpj.2011.10.043
22. Riemann I, Le Harzic R, Mpoukouvalas K, Heimann A, Kempski O, Charalampaki P (2012) Sub-cellular tumor identification and markerless differentiation in the rat brain in vivo by multiphoton microscopy. Lasers Surg Med 44(9):719–725. doi:10.1002/lsm.22079
23. Yu Y, Lee AM, Wang H, Tang S, Zhao J, Lui H, Zeng H (2012) Imaging-guided two-photon excitation-emission-matrix measurements of human skin tissues. J Biomed Opt 17(7):077004. doi:10.1117/1.JBO.17.7.077004
24. Chen AC, McNeilly C, Liu AP, Flaim CJ, Cuttle L, Kendall M, Kimble RM, Shimizu H, McMillan JR (2011) Second harmonic generation and multiphoton microscopic detection of collagen without the need for species specific antibodies. Burns 37(6):1001–1009. doi:10.1016/j.burns.2011.03.013
25. Zhu X, Zhuo S, Zheng L, Jiang X, Chen J, Lin B (2011) Quantification of scar margin in keloid different from atrophic scar by multiphoton microscopic imaging. Scanning 33(4):195–200. doi:10.1002/sca.20230
26. Meek K (1981) The use of glutaraldehyde and tannic acid to preserve reconstituted collagen for electron microscopy. Histochemistry 73(1):115–120
27. Collins JS, Goldsmith TH (1981) Spectral properties of fluorescence induced dy glutaraldehyde fixation. J Histochem Cytochem 29(3):411–414
28. Adur J, Pelegati VB, de Thomaz AA, D'Souza-Li L, Assunção Mdo C, Bottcher-Luiz F, Andrade LA, Cesar CL (2012) Quantitative changes in human epithelial cancers and osteogenesis imperfecta disease detected using nonlinear multicontrast microscopy. J Biomed Opt 17(8):081407–081401. doi:10.1117/1.JBO.17.8.081407
29. Fritze O, Schleicher M, König K, Schenke-Layland K, Stock U, Harasztosi C (2010) Facilitated noninvasive visualization of collagen and elastin in blood vessels. Tissue Eng Part C Methods 16(4):705–710. doi:10.1089/ten.TEC.2009.0309
30. Alperin M, Moalli PA (2006) Remodeling of vaginal connective tissue in patients with prolapse. Curr Opin Obstet Gynecol 18(5):544–550
31. Lin SY, Tee YT, Ng SC, Chang H, Lin P, Chen GD (2007) Changes in the extracellular matrix in the anterior vagina of women with or without prolapse. Int Urogynecol J Pelvic Floor Dysfunct 18(1):43–48. doi:10.1007/s00192-006-0090-1
32. Meijerink AM, van Rijssel RH, van der Linden PJ (2012) Tissue composition of the vaginal wall in women with pelvic organ prolapse. Gynecol Obstet Invest 75(1):21–27. doi:10.1159/000341709
33. Boulesteix T, Pena AM, Pagès N, Godeau G, Sauviat MP, Beaurepaire E, Schanne-Klein MC (2006) Micrometer scale

ex vivo multiphoton imaging of unstained arterial wall structure. Cytometry A 69(1):20–26. doi:10.1002/cyto.a.20196

34. Le TT, Langohr IM, Locker MJ, Sturek M, Cheng JX (2007) Label-free molecular imaging of atherosclerotic lesions using multimodal nonlinear optical microscopy. J Biomed Opt 12(5):054007. doi:10.1117/1.2795437
35. Schenke-Layland K, Stock UA, Nsair A, Xie J, Angelis E, Fonseca CG, Larbig R, Mahajan A, Shivkumar K, Fishbein MC, MacLellan WR (2009) Cardiomyopathy is associated with structural remodelling of heart valve extracellular matrix. Eur Heart J 30(18):2254–2265. doi:10.1093/eurheartj/ehp267